UCRL-JRNL-203051

Spectroscopic properties of Novel Aromatic Metal Clusters: NaM4 (M=Al, Ga, In) and their cations and anions

K. Balasubramanian, Cunyuan Zhao

March 19, 2004

Journal of Chemical Physics

Spectroscopic properties of Novel Aromatic Metal Clusters: NaM_4 (M=Al, Ga, In) and their cations and anions

Cunyuan Zhao

Center for Image Processing and Integrated computing, University of California Davis, Livermore, CA 94550

K. Balasubramanian*

Center for Image Processing and Integrated Computing, University of California Davis, Livermore, CA 94550; University of California, Chemistry and Material Science Directorate, Lawrence Livermore National Laboratory Livermore, California 94550; and Glenn T Seaborg Center, Lawrence Berkeley Laboratory, University of California, Berkeley, CA 94720

The ground and several excited states of metal aromatic clusters, namely NaM_4 and $NaM_4^{\pm}$ (M=Al, Ga, In) clusters have been investigated by employing complete active-space self-consistent-field (CASSCF) followed by Multi-reference singles and doubles configuration interaction (MRSDCI) computations that included up to 10 million configurations and other methods. The ground states NaM_4^- of aromatic anions are found to be symmetric C_{4v} ($^1A_1$) electronic states with ideal square pyramid geometries. While the ground state of $NaIn_4$ is also predicted to be a symmetric C_{4v} ($^2A_1$) square pyramid, the ground state of the $NaAl_4$ cluster is found to have a C_{2v} ($^2A_1$) pyramid with a rhombus base and the ground state of $NaGa_4$ possesses a C_{2v} ($^2A_1$) pyramid with a rectangle base. In general these structures exhibit 2 competing geometries, viz., an ideal C_{4v} structure and a distorted rhomboidal or rectangular pyramid structure (C_{2v}). All of the ground states of the

* The author to whom correspondence should be addressed at kbala@ucdavis.edu

NaM_4^+ (M=Al, Ga, In) cations are computed to be C_{2v} ($^3A_2$) pyramids with rhombus bases. The equilibrium geometries, vibrational frequencies, dissociation energies, adiabatic ionization potentials, adiabatic electron affinities for the electronic states of NaM_4 (M=Al, Ga, In) and their ions are computed and compared with experimental results and other theoretical calculations. On the basis of our computed excited states energy separations, we have tentatively suggested assignments to the observed X and A states in the anion photoelectron spectra of Al_4Na^- reported by Li et al. The X state can be assigned to a C_{2v} ($^2A_1$) rhomboidal pyramid. The A state observed in the anion spectrum is assigned to the first excited state ($^2B_1$) of the neutral $NaAl_4$ with the C_{4v} symmetry. The assignments of the excited states are consistent with the experimental excitation energies and the previous green's function based methods for the vertical transition energy separations between the X and A bands.

I. INTRODUCTION

The concept of aromaticity has been the subject of many studies for years, but recent studies have resurrected the concept to encompass unconventional metal aromaticity[1-15]. Although aromaticity is traditionally associated with organic compounds containing 4n+2 delocalized π-electrons, recent studies by Wang and coworkers[7-13,15] as well as Schleyer and coworkers[1-2,4] have demonstrated that main group metal clusters can exhibit planar aromatic character. These authors have demonstrated the existence of stable group (13) metal clusters anions such as Al_4^{2-}, Ga_4^{2-}, In_4^{2-}, etc., by gas-phase isolation of $NaAl_4^-$, $NaGa_4^-$, $NaIn_4^-$, etc[7-13,15]. It is also very interesting to find species such as Al_4^{2-}, Ga_4^{2-}, In_4^{2-}, since dianions of small clusters are not expected to be unusually stable in the gas-phase, as coulomb repulsion has to be overcome by the unusual stability of these species. Combined experimental and theoretical studies of Wang and coworkers[7-13,15] have demonstrated that these species are not only stable but they exhibit near-square planar forms so that when Na^+ is bound to these, square pyramidal C_{4v} structures are obtained for $NaAl_4^-$, $NaGa_4^-$ and $NaIn_4^-$. While multiply charged main group cluster anions have been known in aqueous solution, and they are also constituents of solids (zintl ions), it is unusual to find such multiply charged cluster ions in the gas-phase. Moreover these dianions are found to be planar aromatic[1-15] in contrast to other main group clusters[16-23], which exhibit three-dimensional structures.

Spectroscopy and theoretical studies of main group clusters have received considerable attention in the last two decades[16-23] as they exhibit interesting structures and properties that vary dramatically with cluster sizes. High-resolution spectroscopic studies of such clusters are on the increase due to the ready generation of these species in the gas-

phase with the advent of supersonic jet expansion methods. Smaller clusters are particularly intriguing, as they exhibit interesting variations in geometries and spectroscopic properties. A number of experimental techniques[16,18,20] have been employed to study the low-lying electronic states of these clusters such as anion photoelectron spectroscopy, resonant two-photon ionization, resonance Raman and far IR spectra of matrix-isolated clusters, and so on.

Experimental studies on NaM_4^- clusters with M=Al,Ga and In have been carried out using a laser vaporization technique in conjunction with the anion photoelectron spectroscopy.[7-13,15] Wang and coworkers[7-13,15] have employed the anion photodetachment spectroscopy to observe not only the ground state but also several low-lying excited states of these species. The anion photoelectron spectra have revealed well-resolved peaks labeled X, A, B and C for a number of these species. These authors have measured the vertical detachment energies (VDE) and have also carried out ab initio studies using the DFT, MP2, CCSD and Green's function based OVGF/6-311+G(2df) methods. Other computational methods have also been employed for the lighter clusters.[14]

In this study, we have investigated the ground and excited states of NaM_4 and $NaM_4^{\pm}$ clusters employing complete active-space self-consistent-field (CASSCF) followed by MRSDCI computations that included up to 10 million configurations as well as density functional theory (DFT) with B3LYP functional. The cations of these clusters have not been studied before, while the neutral and anionic species in their excited states have not been investigated using multi-reference techniques such as the CASSCF and MRSDCI methods. Also the exact spin and spatial symmetries of the excited states of the neutral clusters have not been considered. We have optimized the geometries of the electronic states in both the ground and excited states at these levels of theory. On the basis of our

computed results, we have suggested assignments of the observed anion detachment spectra of these species.

II. METHODS OF INVESTIGATION

The geometries for the neutral clusters NaM_4 (M=Al, Ga, In) and their positive and negative ions are considered in three primary structures (Fig. 1). The first is a square pyramid with the sodium atom at the apex, and the four M (M=Al, Ga, In) atoms constituting a square base; the symmetry of the square pyramid is C_{4v} but when the square base distorts it leads to C_{2v} depending on the arrangements as shown in Figs. 1(a) and (b). The second type of structure is a rhomboidal pyramid with an apex sodium atom and the four M (M=Al, Ga, In) atoms rhombus comprising of the base as shown Fig. 1 (c). The third structure is a sodium edge-capped to one side of the M_4 square resulting in a fully planar structure as shown with C_{2v} symmetry, as can be seen from Fig. 1 (d).

The computations of all NaM_4 (M=Al, Ga, In) clusters and their ions were considered in the C_{2v} point group, although some electronic states have higher C_{4v} symmetries. Geometries were fully optimized at the density functional theory (DFT) and complete active-space self-consistent-field (CASSCF) levels. Subsequently, higher-order multireference singles + doubles configuration interaction (MRSDCI) computations were employed at the optimized CASSCF geometries for seeking more accurate energy separations. All of the computations were made with relativistic effective core potentials (RECPs) [22-25] for the Al, Ga, In and Na atoms with the outer $3s^2 3p^1$, $4s^2 4p^1$, $5s^2 5p^1$ and $2s^2 2p^6 3s^1$ shells retained in the valence space, respectively. The RECPs together with the valence (3s3p) Gaussian basis sets were augmented with an additional set of diffuse s and p functions and two sets of six-component 3d, 4d, 5d functions with α_{d1}=0.2181 and

α_{d2}=0.4362 for Al, α_{d1}=0.291 and α_{d2}=0.09 for Ga and α_{d1}=0.1505 and α_{d2}=0.301 for In. The final basis sets for these three atoms are of (4s4p2d) quality. The basis set of the Na atom was also augmented with an additional set of diffuse s and p functions and one set of six-components 3d functions with exponent α_d=0.175, resulting in a (7s5p1d) basis set.

The CASSCF technique that included all valence orbitals was used to generate the molecular orbitals for higher-order MRSDCI calculations. In the CASSCF computations, 21 valence electrons of the NaM_4 (M=Al, Ga, In) clusters for the geometries shown in Figs. 1 (a), (b) and (c) were distributed in all possible ways among 14 active orbitals spanning seven a_1, three each of b_1 and b_2 and one a_2 symmetries. For the capped-square planar geometry shown in Fig.1 (d), all 21 electrons of the NaM_4 (M=Al, Ga, In) clusters were distributed in all possible ways among 14 active orbitals, which were composed of eight a_1, four b_2 and two b_1. A quasi-Newton-Raphson method was utilized for the geometry optimization of the electronic states of these species. We have also employed the DFT with the B3LYP functional for the ground states and most excited states.

The MRSDCI computations included all configurations in the CASSCF with absolute coefficients $\geq$ 0.07 as reference configurations. These computations included single and double excitations from these reference configurations. Multireference Davison correction technique for the uncoupled quadruple clusters to the MRSDCI energies was invoked and the resulting energy separation was labeled as MRSDCI+Q. The MRSDCI included up to 10 000 000 configurations.

The CASSCF/MRSDCI calculations were made using a modified version of ALCHEMY II codes [26] as modified by one of the authors [27-28] to include relativistic ECPs (RECPs) and more recently to extend the symbolic CI technique[28]. While the CASSCF

geometry optimization was made using the GAMESS[29] package, the DFT/B3LYPcomputations were carried out using the Gaussian 98 [30] codes.

III. RESULTS AND DISCUSSION

Figure 1 illustrates the actual geometries of the various structures considered for NaM_4 (M=Al, Ga, In) clusters. Tables I and II show the optimized geometries of the ground and low-lying excited states of the neutral, anionic and cationic species for NaM_4 that have C_{4v} or C_{2v} symmetries at the CASSCF and DFT levels. As can be seen from Tables I and II, the DFT equilibrium geometries are very close to the CASSCF geometries for the bonded atoms, but the M-Na (M=Al, Ga, In) bond lengths differ by as much as 0.4 Å in some of the low-lying excited states. The B3LYP harmonic vibrational frequencies and IR intensities (in parentheses) for the low-lying states of NaM_4 (M=Al, Ga, In) and their ions shown in Table III confirm that the reported geometries of most of the electronic states are stable minima in Tables I and II, while only a few electronic states with one or two imaginary frequencies are found to be transition states or second-order saddle points.

Table IV shows the energy separations of the low-lying electronic states of the neutral, cationic and anionic species of NaM_4 (M=Al, Ga, In) at the CASSCF, MRSDCI, MRSDCI+Q and DFT levels. The energies were obtained at the optimized geometries shown in Tables I, II and Figure 1 with the square pyramid structure in Fig. 1(a) (C_{4v}), the rectangular pyramid shown in Fig 1(b) (C_{2v}), the rhomboidal pyramid (Fig. 1(c), C_{2v}), and the capped-square planar structure. As can be seen from Table IV, in general there is a good agreement between the DFT and MRSDCI or MRSDCI+Q energies for most of the states but there are differences, especially for some excited states of the edge-capped square planar structure for the neutral NaM_4 (M=Ga, In) species. We consider the MRSDCI or MRSDCI+Q results to be the most accurate as they include singles + doubles

correlation from a multireference set of configurations. The CASSCF results are not expected to be accurate for energy separations of the excited states, as the method does not include dynamic electron correlation effects. The results of all the tables will be discussed in the ensuing sections where each of the species will be considered individually. Table V shows the energetics of various reaction pathways while Table VI comprises of our computed vertical energy separations compared the experimental results and the previous vertical energy separations.

A. $NaAl_4^-$, $NaAl_4^+$ and $NaAl_4$

1. Electronic States, geometries and energy separations

At all four levels of theory, CASSCF, MRSDCI, MRSDCI+Q and DFT/B3LYP combined with the basis set (4s4p2d) for Al and (7s5p1d) for Na, the ground state of $NaAl_4^-$ was found to have a singlet C_{4v} ($^1A_1$) structure with a square pyramid geometry as can be seen from Tables I, II, IV, and Figure 1(a). The square pyramid can be interpreted as a Na^+ cation coordinated to a square planar Al_4^{2-} unit. The harmonic frequency calculation shows that the square pyramid is a true minimum. Our computed geometries are in excellent agreement with the previous CCSD (T)/6-311+G* optimizations[7] in which the Al-Al and Al-Na bond lengths are predicted to be 2.60 and 3.15 Å. In addition, consistent with the previous work[7], we have also found a fully planar structure as one of the low-lying isomers for the Al_4Na^- species. The structure is an edge-capped square planar one (C_{2v}, $^1A_1$, Fig. 1(d)) with the Na^+ cation coordinated to the edge of a square planar Al_4^{2-} unit.. The CCSD (T)/6-311+G* method of calculations[7] yielded geometries that are in good agreement with our CASSCF and DFT geometries with our RECPs and basis sets. At all four levels of theory, namely, CASSCF, MRSDCI, MRSDCI+Q and DFT/B3LYP, the C_{4v} square pyramid was found to be more stable than the edge-capped planar structure by

0.2, 0.537, 0.265 and 0.263 eV, respectively, consistent with the previous CCSD (T)/6-311+G (2df) calculations[7] (7.6 kcal/mol or 0.329 eV). All the above-mentioned general consistencies suggest that our calculated results are reliable for studying the geometries and spectroscopic properties of the low-lying excited electronic states of NaM_4 (M=Al, Ga, In) and their ions.

While the square pyramidal C_{4v} structure is found to be the global minimum for the $NaAl_4^-$ anion, the ground state of the neutral $NaAl_4$ species is predicted to be a slightly distorted pyramid ($^2A_1$, C_{2v}), namely a rhomboidal pyramid with a rhombus base at both CASSCF and DFT levels. The state arises from the removal of an electron from the closed shell a_1 orbital (HOMO) of the anion $NaAl_4^-$ species. This would result in a $^2A_1$ state for $NaAl_4$. The two opposite Al atoms in the square base move closer, while the other two move apart slightly, forming the rhombus base due to the rhomboidal distortion.

The first excited state of $NaAl_4$ is a $^2B_1$ state with a C_{4v} structure similar to the anion ground state $NaAl_4^-$ (except that the bond distances differ slightly), and thus the excitation from the anion ground state to the $^2B_1$ state does not involve large geometry changes. The main reason for the very close energy separation between the ground and first excited states is that the $^2B_1$ state with the C_{4v} structure arises from the removal of an electron from the closed shell b_1 orbital (HOMO-1) of the anion $NaAl_4^-$ and the b_1 orbital is nearly degenerate with the a_1 HOMO orbital of $NaAl_4^-$. The second excited state of $NaAl_4$ is a $^4B_2$ state with a C_{2v} rhomboidal pyramidal geometry, as shown in Figure 1(c). The state arises from the Jahn-Teller distortion of the corresponding E electronic state with a C_{4v} symmetry, which distorts the square into a rhombus base. The geometry of the rhombus base for the $^4B_2$ state can also be visualized as two fused Al_3 triangles. We have also found the other two low-lying electronic states for the edged-capped planar species,

namely $^2B_1$ and $^2A_1$ states, which are quite similar to the $^1A_1$ square planar structure with the C_{2v} symmetry. The geometries of the base in these two states changes slightly compared to the $^1A_1$ (C_{4v}) square planar structure of the anion.

The ground state of the $NaAl_4^+$ cation is predicted to be a $^3A_2$ state with a C_{2v} rhomboidal pyramid as shown Figure 1(c). The electronic configuration for $NaAl_4^+$ ion is $1a_1^{2\cdots}5a_1^{2}1b_1^{2}1b_2^{2}2b_1^{2}1b_2^{2}1a_2^{1}6a_1^{1}$. The B3LYP vibrational frequencies shown in Table III confirm that this is a true minimum without any imaginary frequencies. However, for the $^1A_1$ state this C_{2v} rhomboidal pyramid structure is found to be a transition state with an imaginary frequency, as shown in Table III though the geometry of the state is quite similar to that of the $^3A_2$ ion. The $^1A_1$ state with a C_{4v} square pyramid structure is computed to have two imaginary frequencies, suggesting a second-order saddle point.

2. Dissociation energy, ionization potentials and adiabatic electron affinities

The dissociation energy to separate $NaAl_4^-$ into Al_4^- and Na, that is,

$$NaAl_4^- (C_{4v}, {}^1A_1) \rightarrow Al_4^- (D_{4h}, {}^2A_{1g}) + Na ({}^2S)$$

is computed as 1.561 and 1.420 eV at the MRSDCI and B3LYP levels, respectively, as can be seen from Table V. In all of the MRSDCI dissociation energy calculations, the Na atom was always placed above the center of the Al_4 square base at 10 Å, that is, such computations were carried out as a supermolecular computation. We have computed dissociation energy for separating $NaAl_4^-$ into Al_4^{2-} and Na^+ as 8.504 eV at the DFT level. This suggests ionic interaction between the Al_4^{2-} unit and Na^+. A simple point charge electrostatic model at the computed equilibrium distance gives an interaction energy close to ~ 9 eV. This suggests that most if the interaction is ionic with some back transfer from Al_4^{-2} to Na^+. It is anticipated that this interaction arises from the characteristics of

aromaticity for Al_4^{2-} in that it possesses two completely delocalized π electrons, which satisfy the (4n+2) electron-counting rule for aromatic compounds.

The dissociation energy to separate $NaAl_4$ into Al_4 and Na

$$NaAl_4\ (C_{2v},\ ^2A_1) \rightarrow Al_4\ (C_{2v},\ ^1A_1) + Na\ (^2S)$$

was computed as 1.799 and 1.984 eV at the MRSDCI and B3LYP levels, respectively, as shown in Table V. Note that the neutral Al_4 base is no longer a C_{4v} square but a rhombus with C_{2v} symmetry.

Likewise, the dissociation energy to separate Al_4Na^+ into Al_4 and Na^+

$$NaAl_4^+\ (C_{2v},\ ^3A_2) \rightarrow Al_4\ (C_{2v},\ ^3A_1) + Na^+\ (^1S)$$

was computed as 1.296 and 1.273 eV at the MRSDCI and B3LYP levels, respectively (Table V).

At the MRSDCI+Q and DFT/B3LYP levels, the adiabatic ionization potentials for $NaAl_4$ are computed as 5.703 and 5.793 eV, respectively. At different levels of theory, we have also computed the adiabatic electron affinities for $NaAl_4$. As seen from Table IV, at the MRSDCI+Q and DFT/B3LYP levels, the adiabatic electron affinities are computed as 1.441 and 1.804 eV, respectively.

3. Comparison with photoelectron spectra of $NaAl_4^-$.

Li et al.[7] have reported the anion photoelectron spectra of MAl_4^- (M=Li, Na, Cu) clusters. The anion photoelectron spectrum of $NaAl_4^-$ obtained using a laser wavelength 355nm showed that there are four prominent peaks located subsequent to the detachment of the electron. The four bands are located at the binding energies (BE) of 2.04, 2.09, 2.70, 2.96 eV, identified with the X, A, B, and C states, respectively. The authors also performed optimizations at the B3LYP, MP2 and CCSD (T)/6-311+G* levels for the global minimum and low-lying isomers of the anion $NaAl_4^-$. At their highest level of theory (CCSD (T)/6-

311+G (2df)), they have predicted that the pyramidal structure is favored by 7.6 kcal/mol over the edge-capped planar structure. They have also assigned the spectra using the orbital energies computed by the outer valence Green function (OVGF) method, incorporated into GAUSSIAN 98. In the current study we have actually computed the low-lying excited electronic states with spin multiplicities and spatial symmetries. The geometries were also optimized for each of the excited states considered here by us. This may explain the excellent agreement that was obtained previously for all three anions including Al_4Na^- between the theoretical vertical detachment energies (VDEs) of the pyramidal ground state structures and the experimental spectra, while the previously predicted VDEs[7] for the low-lying planar isomers do not agree as well with the experimental data. Therefore, Li et al.[7] have concluded that the square pyramidal structures (C_{4v} symmetry) are the global minima for all three MAl_4^- (M=Li, Na, Cu) species. Table VI compares our computed vertical energy separations for the various electronic states with the corresponding experimental values[7] and the previous theoretical values[7]. As seen from Table VI, the agreement between our computed vertical energies and experiment is quite good thus confirming that the differences between our adiabatic results and experiment is primarily due to geometrical relaxations.

While the ground state of the $NaAl_4^-$ anion was established unambiguously by experiment and theoretical calculations as a square pyramidal C_{4v} structure, less information is available on the ground and excited states for the neutral species $NaAl_4$. As indicated before, the ground state of $NaAl_4$ is predicted to have a pyramidal structure with a rhombus base (C_{2v} symmetry), as can be seen from Tables I, II and IV. The experimental adiabatic electron affinities (ADEs)[7] can be taken from the onset of the spectrum of anion $NaAl_4^-$ as 1.8 eV. This is in good agreement with our computed ADEs at four levels of

theory. The DFT method predicted the ADE as 1.804 eV, which is in an excellent agreement with the experimental data. However, the CASSCF, MRSDCI and MRSDCI+Q methods underestimate the ADEs for $NaAl_4$ as shown in Table IV.

The photoelectron spectrum obtained by Li *et al.*[7] exhibits four bands at VDEs of 2.04, 2.09, 2.70, 2.96 eV, assigned to X, A, B, C, respectively. The data suggest that there are three excited states, which lie at 0.05, 0.66 and 0.92 eV above the ground state, respectively. We have tentatively assigned the bands X and A of the photoelectron spectrum on the basis of our computed energies and harmonic vibrational frequencies. The band X shown at BE=2.04 eV is unambiguously assigned to the transition from the anion $NaAl_4^-$ to the neutral $^2A_1$ ground state of $NaAl_4$. The state is slightly distorted from an ideal C_{4v} pyramid, as discussed in previous section. The lowest excited state (A) that we computed is the $^2B_1$ (C_{4v}) state with a square pyramidal geometry, which is calculated at 0.114 and 0.169 eV at the MRSDCI+Q and DFT levels. Considering an error bar of 0.05 eV for the experimental VDEs, our calculated results are in good agreement with the experimental first excitation energy of 0.05 eV. Our calculated first excitation energy also agrees well with the theoretical VDE separation of 0.13 eV between the X and A bands obtained by the OVGF method. Considering that the $NaAl_4^-$ anion possess a C_{4v} pyramidal structure and the $^2A_1$ ground state of the neutral $NaAl_4$ is slightly distorted from an ideal C_{4v} square pyramidal structure, the best fit for the band A is the $^2B_1$ state with a C_{4v} pyramidal structure. Moreover this state arises from the removal of an electron from the b_1 (HOMO-1) orbital, consistent with the excellent agreement between the experimental and theoretical VDEs obtained from the spectra and the OVGF calculations of Li et al.[7] for the A band. Moreover, as seen from Table III, all of the vibrational frequencies of the $^2B_1$ (C_{4v}) state are real confirming our assignment. Furthermore on the basis of good agreement that

we find in Table VI for the vertical energy separations for Ga_4Na, we conclude that these assignments are reasonable. No assignment has been suggested earlier for the A band of the observed spectrum.

The B and C bands with experimental excitation energies 0.66 and 0.92 eV do not fit any of our computed adiabatic excitation energies, as most of our low-lying excited states are in the region of 0.15-0.4 eV. Considering that the experimental excitation is vertical and our optimized geometries distort significantly from the ideal square pyramidal C_{4v} structure, it is fully understandable that our computer energy separations are lower than experimental values. We thus cannot make any definitive assignments for the B and C bands without further gas-phase neutral experimental evidence even though the predicted second excited states $^4B_2$ with a C_{2v} rhomboidal pyramid is only 0.217 eV above the neutral ground state at the MRSDCI+Q level.

B. $NaGa_4^-$, $NaGa_4^+$ and $NaGa_4$

1. Electronic States, geometries and energy separations

Analogous to $NaAl_4^-$, the ground state of $NaGa_4^-$ was found to have a $^1A_1$ C_{4v} square pyramidal structure. The square pyramid is composed of a Na^+ cation coordinated to a square planar Ga_4^{2-} unit. The harmonic frequency calculation shows that the square pyramid structure is a true minimum. It is surprising that the Ga-Ga bond lengths in the dianion Ga_4^{2-} are a bit shorter than those of lighter aluminum analogue Al_4^{2-}. However, this is consistent with the findings of Li et al[7] and Kuznetsov et al.[15] In addition, we have also found a fully planar structure as one of the low-lying isomers for the $NaGa_4^-$ species. The structure is an edge-capped square planar one (C_{2v}, $^1A_1$, Figure 1(d)) with the Na^+ cation capped to the edge of a square planar Ga_4^{2-} unit. As can be seen from Table III, the harmonic frequency calculations show that this fully planar structure is a minimum. At the CASSCF, MRSDCI, MRSDCI+Q and DFT/B3LYP levels, the C_{4v} square pyramid was found to be more stable than the edge-capped planar structure, similar to the aluminum analogue.

We have found that in contrast to $NaAl_4$, the ground state of the neutral $NaGa_4$ is hard to determine due to a very shallow potential energy surface of the $NaGa_4$ cluster. As can be seen from Tables I to II, at the CASSCF and DFT levels, the ideal square pyramid (Figure 1(a), $^2A_1$, C_{4v}) and the rectangular pyramid (Figure 1(b), $^2A_1$, C_{2v}) appear to have the lowest energy. At all four levels of theory, CASSCF, MRSDCI, MRSDCI+Q and DFT/B3LYP, the energies of the two structures are almost the same. Among the four levels of theory, the MRSDCI+Q method predicts the largest energy separation for the two structures, i.e., the C_{2v} structure with a rectangle base is favored by 0.08 eV. The zero point corrected DFT/B3LYP energies also favor this C_{2v} structure by 0.03 eV. Furthermore, as

can be seen from Table III, the DFT/B3LYP harmonic frequency calculations show that the C_{2v} structure has no imaginary frequencies, whereas the ideal C_{4v} square pyramid possesses one small imaginary frequency ($43.2i$ cm^{-1}, a_2). It should be noted that the geometry differences between the C_{2v} and C_{4v} structures are very small in that the averaged Ga-Ga and Ga-Na bond lengths of the C_{2v} structure with a rectangle base are almost same as those of the ideal C_{4v} structure as shown in Tables I and II. We, therefore, tentatively assign the ground state of neutral $NaGa_4$ to a $^2A_1$ C_{2v} structure with a rectangular base although the ideal C_{4v} structure cannot be definitely ruled out due to the very small energy separation between the two structures. The $^2A_1$ state arises from the removal of an electron from the closed shell a_1 orbital (HOMO) of the $NaGa_4^-$ anion.

The first excited state of $NaGa_4$ is a $^2B_1$ state with a C_{4v} structure similar to the $NaGa_4^-$ anion's ground state (except that the bond distances differ slightly), and thus the excitation from the anion ground state to the $^2B_1$ state does not involve large geometry changes. The energy of the lowest excited state 0.242 eV above the C_{2v} ground state at the MRSDCI+Q level. The next excited state of $NaGa_4$ is a $^4B_2$ state with a C_{2v} rhomboidal pyramid as shown in Figure 1(c). The geometries of the rhombus base for the $^4B_2$ state can be visualized as two fused Ga_3 triangles. We have also found two other low-lying electronic states for the edged-capped planar species, namely $^2B_1$ and $^2A_1$ states, which are quite similar to the $^1A_1$ square planar structure of the anion with C_{2v} symmetry. The geometries of the square base in these two states change slightly compared to the $^1A_1$ square planar structure. As can be seen from Table III, the harmonic frequency calculation shows that the square pyramid is a true minimum.

Our calculated vibrational frequencies are in excellent agreements with the previous B3LYP/6-311+G* frequencies.[15] For the C_{4v} pyramidal structure of $NaGa_4^-$, our

optimized geometries are in excellent agreements with the previous B3LYP/6-311+G* optimizations[15] in which the Ga-Ga and Ga-Na bond lengths are calculated to be 2.580 and 3.134 Å. For the C_{2v} planar structure of $NaGa_4^-$, the previous B3LYP/6-311+G* calculations[15] yielded the corresponding bond lengths as 2.611, 2.480, 2.563 and 2.914 Å, in good agreement with our CASSCF and DFT geometries with the RECP basis set. At all four levels of theory, namely, CASSCF, MRSDCI, MRSDCI+Q and DFT/B3LYP levels, the C_{4v} pyramidal structure was found to be more stable than the C_{2v} planar structure similar to the aluminum analogue. The energy gap is also consistent with the previous CCSD (T)/6-311+G (2df) calculations[15]

The ground state of the $NaGa_4^+$ ion is a $^3A_2$ state with a C_{2v} rhomboidal pyramid structure shown in Figure 1(c). The B3LYP vibrational frequencies shown in Table III confirm that this is a true minimum without any imaginary frequencies. However, the $^1A_1$ state with an ideal C_{4v} square pyramid is found to be a transition state with an imaginary frequency ($103i$ cm^{-1}, b_1) as can be seen from Table III. This state would thus undergo a distortion in different directions along one of the sides of the square base and would result in a structure with a rectangular base, similar to the neutral ground state. The Frequencies show that this is a true minimum.

2. Dissociation energy, ionization potentials and adiabatic electron affinities

The dissociation energy to separate $NaGa_4^-$ into Ga_4^- and Na, that is,

$$NaGa_4^- (C_{4v}, {}^1A_1) \rightarrow Ga_4^- (D_{4h}, {}^2A_{1g}) + Na ({}^2S)$$

is computed as 1.528 and 1.429 eV at the MRSDCI and B3LYP levels, respectively, as shown in Table V. Another dissociation pathway for decomposing $NaGa_4^-$ into Ga_4^{2-} and Na^+ was computed to be 8.591 eV at the DFT level. The dissociation energy to separate the neutral $NaGa_4$ into Ga_4 and Na

$$NaGa_4\ (C_{2v},\ ^2A_1) \rightarrow Ga_4\ (D_{4h},\ ^1A_{1g}) + Na\ (^2S)$$

was computed as 1.799 and 1.984 eV at the MRSDCI and B3LYP levels, respectively, as shown in Table V. Finally, the dissociation energy to separate $NaGa_4^+$ into Ga_4 and Na^+

$$NaGa_4^+\ (C_{2v},\ ^3A_2) \rightarrow Ga_4\ (D_{4h},\ ^3A_{1g}) + Na^+\ (^1S)$$

was computed as 1.296 and 1.273 eV at the MRSDCI and B3LYP levels, respectively, as shown in Table V.

At the highest MRSDCI+Q level, the adiabatic ionization potentials for $NaGa_4$ is computed as 5.421 eV. At different levels of theory, we have also computed the adiabatic electron affinities for $NaGa_4$ (see Table IV).

3. Comparison with photoelectron spectra of $NaGa_4^-$.

Next we compare our computed energy separations with the photoelectron spectra of Kuznetsov et al.[15]. At their highest level of theory (CCSD (T)/6-311+G (2df)), Kuznetsov et al have predicted that the C_{4v} pyramidal structure is more stable than the C_{2v} planar structure by 5.6 kcal/mol for the anion Ga_4Na^-. Analogous to their earlier work[7] on $NaAl_4^-$ ion, they have also used the OVGF method to obtain the orbital energies in order to provide assignments to the observed peaks. They have obtained reasonable agreement for the two anions including $NaGa_4^-$ between the theoretical vertical detachment energies (VDEs) of the C_{4v} pyramidal structure and the experimental spectra, while the predicted VDEs of the low-lying C_{2v} isomers were found to be uniformly lower than those of the C_{4v} pyramidal structure. This led them to conclude that the C_{4v} structure is the ground state for both anions.

It is evident that the ground state of the anion $NaGa_4^-$ was established unequivocally by experiment and theoretical calculations as a C_{4v} pyramid. However, less information is available on the ground and excited states for the neutral species $NaGa_4$. As

indicated before, the ground state of $NaGa_4$ is predicted to have a C_{2v} square pyramid with a rectangle base. The experimental adiabatic electron affinities (ADEs) can be taken from the onset of the photoelectron spectrum of anion $NaGa_4^-$ as 1.7 eV. We have computed the ADEs at four levels of theory, and at the highest MRSDCI+Q level, our computed ADE is 1.708 eV, in excellent agreement with the experimental data. The predicted ADEs by both the MRSDCI and DFT methods also agree quite well, as can be seen from Table IV.

The photoelectron spectrum of $NaGa_4^-$ obtained by Kuznetsov et al.[15] exhibits four bands at 1.90, 2.02, 2.58, 3.73 eV, namely, X, A, B, C, respectively, which suggest that there are three excited states that lie at 0.12, 0.68 and 1.83 eV above the X ground state. We have shown our computed vertical energy separations in Table VI for the excited states as computed at the anion's optimized geometry. As can be seen from Table VI, the agreement between our computed vertical energy separations and the experiment is excellent. We have tentatively assigned the bands X, A of the photoelectron spectrum on the basis of our computed energies and harmonic vibrational frequencies. The band X at BE=1.90 eV is unambiguously assigned to the transition from the anion $NaGa_4^-$ to the neutral $^2A_1$ ground state of $NaGa_4$. The neutral state is a C_{2v} pyramid [Fig. 1(b)] with a rectangle base, which is slightly distorted from an ideal C_{4v} pyramid, as discussed in the previous section. The lowest excited state that we have computed is the $^2B_1$ (C_{4v}) state with a square pyramidal geometry, which is computed at 0.242 at the MRSDCI+Q level. Considering that the experimental error bar is 0.06 eV for the VDEs, our calculated results are in excellent agreement with the experimental first excitation energy of 0.12 eV. Our calculated first excitation energy also agrees well with the theoretical VDE separation of 0.15 eV between the X and A bands obtained by the OVGF method.[15] Considering that the $NaGa_4^-$ anion has a C_{4v} pyramidal structure and the $^2A_1$ ground state of the neutral $NaGa_4$ is

slightly distorted from an ideal C_{4v} square pyramidal structure, the best fit for the A band is the $^2B_1$ state with a square C_{4v} pyramidal structure.

Analogous to $NaAl_4^-$, our computed adiabatic results for the excited states do not fit well with the observed B and C bands with the experimental excitation energies of 0.66 and 0.92 eV. Since the experimental excitation is vertical and our optimized geometries distort significantly from the ideal square pyramidal C_{4v} structure, it is difficult to make definitive assignments for these bands. But our vertical excitation energies compare favorably with the experiment(see, Table VI).

C. $NaIn_4^-$, $NaIn_4^+$ and $NaIn_4$

1. Electronic States, geometries and energy separations

The ground state of $NaIn_4^-$ is similar to the lighter analogs in that it is a C_{4v} ($^1A_1$) square pyramidal structure. As seen from Table III, all of the computed frequencies are real, which confirm that the square pyramid is a genuine minimum. The bond lengths are much longer than those of the Al and Ga clusters whereas the bond lengths change insignificantly in going from the Al to Ga clusters. This may be attributed to the similar atomic radii of Al and Ga while indium's atomic radius is much larger than those of Al and Ga. In addition, we have also found a fully planar structure as one of the low-lying isomers for the $NaIn_4^-$ species. The vibrational frequency calculations show that this fully planar structure is a true minimum. The geometries of the In_4^{2-} unit change slightly in going from the square pyramid to the planar structure. At the MRSDCI+Q level, the C_{4v} square pyramid was computed to be more stable than the edge-capped planar structure by 0.567 eV. It appears that the edge-capped planar structure becomes less stable as one goes down the column of the periodic table from Al to In.

In contrast to the lighter analogues, the ground state of $NaIn_4$ is definitely an ideal square pyramid (Figure 1(a), $^2A_1$, C_{4v}). It seems that the symmetric C_{4v} structure becomes more stable as one moves from $NaAl_4$ to $NaIn_4$. The DFT/B3LYP vibrational frequency calculations show that the C_{4v} structure has no imaginary frequencies confirming that it is a true minimum. The $^2A_1$ state arises from the removal of an electron from the closed shell a_1 orbital (HOMO) of the anion $NaGa_4^-$. The geometry of the $^2A_1$ state is quite similar to that of the anionic cluster.

The first excited state of $NaIn_4$ is predicted to be a $^2B_1$ state with a C_{4v} structure similar to the neutral and anion ground states of $NaGa_4$ and $NaGa_4^-$. It seems that the excitations from the anion ground state to both $^2A_1$ and $^2B_1$ states do not involve large geometry changes for $NaIn_4$. The energy of the first excited state is 0.103 eV relative to the ideal C_{4v} ground state at the MRSDCI+Q level. The second excited state of In_4Na is a $^4B_2$ state with a C_{2v} rhomboidal pyramid shown Figure 1(c). We have also found two other low-lying candidates for the electronic states with the edged-capped planar structures, namely the $^2B_1$ and $^2A_1$ states, similar to the lighter analogues, i.e., $NaAl_4$ and $NaGa_4$.

In comparison to the previous work[15] our optimized geometries are in good agreement for the C_{4v} pyramidal structure of $NaIn_4^-$; the previous B3LYP/CEP-121G+spd optimizations[15] yielded the In-In and In-Na bond lengths as 2.96 and 3.37 Å. For the C_{2v} planar structure of $NaIn_4^-$, the previous B3LYP/CEP-121G+spd calculations[15]yielded the corresponding bond lengths as 2.97, 2.85, 2.95 and 3.13 Å, in good agreement with our CASSCF and DFT geometries with RECP basis set. Our computed energy gap (0.3-0.6 eV) between the C_{4v} ground state and the C_{2v} planar state is also consistent with the previous B3LYP/CEP-121G+spd calculations[15] (6.9 kcal/mol or 0.299 eV).

The ground state of the $NaIn_4^+$ ion is a $^3A_2$ state with a C_{2v} rhomboidal pyramid shown in Figure 1(c). The B3LYP vibrational frequencies shown in Table III confirm that it is a true minimum. However, the $^1A_1$ state with an ideal C_{4v} square pyramid is a transition state with an imaginary frequency ($47.8i$ cm^{-1}), as shown in Table III. The state would undergo rhomboidal distortion into the other structure.

2. Dissociation energy, ionization potentials and adiabatic electron affinities

As can be seen from Table V, the dissociation energy for In_4Na^- to separate into In_4^- and Na, that is,

$$NaIn_4^- (C_{4v}, {}^1A_1) \rightarrow In_4^- (D_{4h}, {}^2A_{1g}) + Na ({}^2S)$$

is computed as 1.331 and 1.383 eV at the MRSDCI and B3LYP levels, respectively. The dissociation energy for decomposing In_4Na^- into In_4^{2-} and Na^+ was also computed as 8.307 eV at the DFT level. The dissociation energy to separate $NaIn_4$ into In_4 and Na

$$NaIn_4 (C_{2v}, {}^2A_1) \rightarrow In_4 (D_{4h}, {}^1A_{1g}) + Na ({}^2S)$$

was computed as 1.886 and 1.844 eV at the MRSDCI and B3LYP levels, respectively (see Table V). The dissociation energy of the $NaIn_4^+$ ion into In_4 and Na^+

$$NaIn_4^+ (C_{2v}, {}^3A_2) \rightarrow In_4 (D_{4h}, {}^3A_{1g}) + Na^+ ({}^1S)$$

was computed as 1.029 and 1.253 eV at the MRSDCI and B3LYP levels, respectively.

The adiabatic ionization potential for $NaIn_4$ is computed as 5.272 eV, at the MRSDCI+Q level. At different levels of theory, we have also computed the adiabatic electron affinities for $NaIn_4$.

3. Comparison with photoelectron spectra of $NaIn_4^-$.

Analogous to previous sections where we have compared our computed results with Kuznetsov et al.'s[15] photoelectron spectra, we find that there is a general qualitative agreement although there are quantitative differences originating from vertical versus

adiabatic energy separations. In their calculations, the C_{4v} pyramidal structure is predicted to be more stable than the C_{2v} planar structure by 6.9 kcal/mol for $NaIn_4^-$. They have also computed the *ab initio* orbital energies using the outer valence Green function (OVGF) method and used them to assign the experimental spectra. On the basis of the overall agreement between the photoelectron spectra and the theoretical vertical detachment energies (VDEs) of the C_{4v} pyramidal structure, these authors have concluded that the C_{4v} structure is the ground state for both anions.

As indicated before, the ground state of $NaIn_4$ is predicted to have a C_{4v} pyramidal structure as seen from Tables I, II and IV. The experimental adiabatic electron affinities structure and its ADE can be obtained from the onset of the spectrum of the $NaIn_4^-$ anion as 1.8 eV. Our computed ADE at the MRSDCI+Q level is 1.785 eV, in excellent agreements with the experimental ADE.

Analogous to lighter species, the photoelectron spectrum of $NaIn_4^-$ obtained by Kuznetsov et al.[15] exhibits four bands at 1.93, 2.08, 2.60, 3.95 eV, labeled X, A, B, C, respectively. The data suggest that there are three excited states, which lie at 0.15, 0.67 and 1.02 eV. The band X at BE=1.93 eV is unambiguously assigned to the transition from the anion $NaIn_4^-$ to the neutral $^2A_1$ ground state of $NaIn_4$ with a C_{4v} pyramidal structure. The first excited state is the C_{4v} $^2B_1$ state, which is computed at 0.103 eV at the MRSDCI+Q level. Since the experimental error bar is 0.06 eV for the VDEs, our calculated results are in good agreement with the experimental first excitation energy of 0.15 eV. This result also agrees with the OVGF VDE separation[15] of 0.11 eV between the X and A bands. In this case the agreement between theory and experiment is better since both the anion $NaIn_4^-$ and the neutral $NaIn_4$ species are predicted to have C_{4v} pyramidal structures.

D. Comparison of NaM_4 (M=Al, Ga, In) and their ions

One of the most interesting features of the clusters is their aromaticity [15-19] and integrity of the M_4^{2-} (M=Al, Ga, In) units. Our calculations revealed that all the M_4^{2-} (M=Al, Ga, In) dianions possess perfect square planar structures. The M-M (M=Al, Ga, In) bond lengths are calculated to be 2.618, 2.569 and 2.918 Å, respectively, at the CASSCF level, while the corresponding values are 2.602, 2.566 and 2.904 Å at the DFT level. Inspection of their valence molecular orbitals reveals that the highest occupied molecular orbital (HOMO) is a doubly occupied π orbital. In addition, all three M_4^{2-} (M=Al, Ga, In) dianions possess two delocalized π electrons and follow the (4n+2) π-electron-counting rule for aromatic compounds, confirming all three dianions exhibit characteristics of aromaticity. The square planar M_4^{2-} (M=Al, Ga, In) units undergo small geometrical changes in forming the NaM_4 (M=Al, Ga, In) clusters and their positive and negative ions for most of the low-lying electronic states, either pyramidal or planar structures. The main differences are in the geometries of the bases, which seem to undergo rhomboidal distortions. The similarities among the structures for most of the low-lying electronic states reflect in the energy separations, as shown in Table IV. All the neutral and positive ions exhibit very flat potential energy surfaces and result in very small energy separations for most of the low-lying electronic states.

There are some similarities among the anions NaM_4^- (M=Al, Ga, In), which might be responsible for the structural features of most of the low-lying neutral and cationic electronic states. The a_1 HOMO orbital is mainly $[M_1(p_y)+M_2(p_x)-M_3(p_x)-M_4(p_x)]$, which also includes contributions from the s orbitals of the four M atoms and the p_z orbital of the Na atom. On the other hand, the b_1 (HOMO-1) orbital is mainly $[M_1(p_x)+M_2(p_y)-M_3(p_x)-M_4(p_y)]$, which cannot include any contributions from the s orbitals of M atoms or the

orbitals of sodium atom. This explains why the $^2A_1$ (C_{2v}) ground state of the neutral $NaAl_4$ and $NaGa_4$ clusters distort slightly from the ideal C_{4v} square pyramidal structures. The similarity in the compositions of the HOMO and (HOMO-1) orbitals leads to degenerate orbital energies as inferred from our DFT/B3LYP calculations, and also lead to almost degenerate $^2A_1$ and $^2B_1$ states for the neutral species.

IV. CONCLUSIONS

In this study, we have investigated the equilibrium geometries, vibrational frequencies, adiabatic ionization potentials, adiabatic electron affinities, dissociation energies for separating the NaM_4, $NaM_4^{\pm}$ into M_4^{2-} or M_4^- or M_4 and Na or Na^+ and energy separations of the low-lying electronic states for the NaM_4 (M=Al, Ga, In) clusters and their anions and cations employing state-of-the-art CASSCF followed by MRSDCI computations that included up to 10 million configurations as well as DFT/B3LYP computations. We have found a symmetric $^1A_1$ electronic state with an ideal square pyramidal (C_{4v}) structure as the ground state of NaM_4^- (M=Al, Ga, In) clusters. The ground state of $NaIn_4$ is predicted to be a symmetric C_{4v} square pyramid. On the other hand, the ground state of the $NaAl_4$ cluster was found to have a C_{2v} rhomboidal pyramid, while the ground state of $NaGa_4$ possesses a C_{2v} rectangular pyramid. The ground states of the NaM_4^+ (M=Al, Ga, In) cations were found to be a $^3A_2$ electronic state with C_{2v} rhomboidal pyramid structures. The assignment for the ground state of $NaAl_4^-$ is in accord with the previous CCSD (T)/6-311+G* calculations[7] and the experimental photoelectron spectra[7] of $NaAl_4^-$.

The energy separations for the low-lying doublet and quartet states were computed and compared with the photoelectron spectra of $NaAl_4^-$ of Wang and coworkers.[7] On the basis of our computed energy separations, vibrational frequencies and comparison with the

experimental VDEs, we have assigned the spectra. The neutral $NaAl_4$ is found to have a C_{2v} rhomboidal pyramid geometry while the anion exhibits an ideal C_{4v} square pyramid structure. The A state observed in the anion detachment spectra is assigned to the $^2B_1$ excited state of the neutral $NaAl_4$ with the C_{4v} symmetry. The assignment of the excited state is in good agreement with the experimental excitation energy and the OVGF/6-311+G(2df) VDE separation[15] between the X and A bands. The properties of the $NaGa_4$ and $NaIn_4$ clusters and their positive and negative ions were also computed and discussed.

Acknowledgment

The research at UC Davis was supported by the National Science Foundation under Grant No. CHE-0236434. The work at LLNL was performed in part under the auspices of the US department of Energy by the University of California, LLNL under contract number W-7405-Eng-48

[1]F. Stahl, P. v. R. Schleyer, H. Jiao, H. F. Schaefer, III, H.-H. Cheu, and N. L. Allinger, J. Org. Chem. **67**, 6599(2002); M. K. Cyranski, T. M. Krygowski, A. R. Katritzky, and P. v. R Schleyer, J. Org. Chem. **67**, 1333 (2002)

[2]Y. Yie, H. F. Schaefer III, and J. S. Thrasher, J. Mol. Struct. Theochem. **234**, 247 (1991)

[3]E. D. Bergman and B. Pullman, (editors), Aromaticity, Pseudoaromaticity and Antiaromaticity, Israel Academy of Sciences, Jerusalem, Israel 1971

[4] P. v. R. Schleyer, H. Jiao, N. J. R. v. E. Hommes, V. G. Malkin, and O. Malkina, *J. Am. Chem. Soc.* **119**, 12669 (1997)

[5]P. J. Garratt, Aromaticity ,Wiley, (New York, NY 1986).

[6] V. I. Minkin, M. N. Glukovtrev, and B. Ya. Simkin, Aromaticity and Antiaromaticity Wiley, (New York, NY 1994).

[7] X. Li, A. E. Kuznetsov, H. F. Zhang, A. I. Boldyrev, and L. S. Wang, Science **291**, 859 (2001).

[8] A. I. Boldyrev, X. Li, and L. S. Wang, Angew. Chem. Int. Ed. **39**, 3307 (2000).

[9] X. Li, L. S. Wang, A. I. Boldyrev, and J. Simons, J. Am. Chem. Soc. **121**, 6033 (1999).

[10] L. S. Wang, A. I. Boldyrev, X. Li, and J. Simons, J. Am. Chem. Soc. **122**, 7681 (2000).

[11] G. D. Geske, A. I. Boldyrev, X. Li, and L. S. Wang, J. Chem. Phys. **113**, 5130 (2000).

[12] X. Li, H. F. Zhang, L. S. Wang, A. E. Kuznetsov, N. A. Cannon and A. I. Boldyrev, Angew. Chem. Int. Ed. **40**, 1867 (2001).

[13]A. I. Boldyrev, J. Simons, X. Li, and L. S. Wang, J. Am. Chem. Soc. **121**, 10193 (1999); A. I. Boldyrev, J. Simons, X. Li, W. Chen, and L. S. Wang, J. Chem. Phys. **110**, 8980 (1999).

[14] S. Shetty, D. G. Kanhere, and S. Pal, J. Phys. Chem. **108**, 628 (2004)

[15]A. E. Kuznetsov, A. I. Boldyrev, X. Li and L. S. Wang, J. Am. Chem. Soc. **123**, 8825 (2001)

[16] M. L. Mandich, W. D. Reents, Jr., and V. E. Bondybey, *Main Group Clusters: A review. In Atomic and Molecular Cluster*s, edited by E. Bernstein (Elsevier, New York, 1991).

[17] J. D. Corbett, Angew. Chem. Int. Ed. **39**, 670 (2000).

[18] T. R. Taylor, H. Gomez, K. R. Asmis, and D. M. Neumark, J. Chem. Phys. **115**, 4620 (2001).

[19] K. Balasubramanian and X. L. Zhu, J. Chem. Phys. **115**, 8858 (2001).

[20] K. Balasubramanian, J. Phys. Chem. A **104**, 1969 (2000); Chem. Rev **90**, 93(1990); Chem Rev. **89**, 1801 (1989).

[21] C. Y. Zhao and K. Balasubramanian, J. Chem. Phys. **115**, 3121 (2001); C. Y. Zhao and K. Balasubramanian, ibid. **116**, 3690 (2002); C. Y. Zhao and K. Balasubramanian, ibid. **116**, 10287 (2002)..

[22] K. Balasubramanian, *Relativistic Effects in Chemistry: Part A, Theory and Techniques* (Wiley Interscience, New York, 1997), p. 381.

[23] K. Balasubramanian, *Relativistic Effects in Chemistry: Part B, Applications* (Wiley Interscience, New York, 1997), p. 521.

[24] L. F. Pacios and P. A. Christiansen, J. Chem. Phys. **82**, 2664 (1985).

[25] L. A. LaJohn, P. A. Christiansen, R. B. Ross, T. Atashroo, and W. C. Ermler, J. Chem. Phys. **87**, 2812 (1987).

[26] The major authors of ALCHEMY II are B. Lengsfield, B. Liu and M. Yoshimine

[27] K. Balasubramanian, Chem. Phys. Lett. **127**, 324 (1986).

[28] K. Balasubramanian, J. Chem. Phys **93**, 6585 (1993); J. Chem. Phys. **112**, 7425 (2000); *Chem. Phys. Lett.*, **365**, 413 (2002)

[29] M. W. Schmidt, K. K. Baldridge, J. A. Boatz, S. T. Elbert, M. S. Gordon, J. H. Jensen, S. Koseki, N. Matsunaga, K. A. Nguyen, S. J. Su, T. L. Windus, M. Dupuis, and J. A. Montgomery, J. Comput. Chem. **14**, 1347 (1993).

[30]Gaussian 98, Revision A.7, M. J. Frisch, G. W. Trucks, H. B. Schlegel, G. E. Scuseria, M. A. Robb, J. R. Cheeseman, V. G. Zakrzewski, J. A. Montgomery, Jr., R. E. Stratmann, J. C. Burant, S. Dapprich, J. M. Millam, A. D. Daniels, K. N. Kudin, M. C. Strain, O. Farkas, J. Tomasi, V. Barone, M. Cossi, R. Cammi, B. Mennucci, C. Pomelli, C. Adamo, S. Clifford, J. Ochterski, G. A. Petersson, P. Y. Ayala, Q. Cui, K. Morokuma, D. K. Malick, A. D. Rabuck, K. Raghavachari, J. B. Foresman, J. Cioslowski, J. V. Ortiz, A. G. Baboul, B. B. Stefanov, G. Liu, A. Liashenko, P. Piskorz, I. Komaromi, R. Gomperts, R. L. Martin, D. J. Fox, T. Keith, M. A. Al-Laham, C. Y. Peng, A. Nanayakkara, C. Gonzalez M. Challacombe, P. M. W. Gill, B. Johnson, W. Chen, M. W. Wong, J. L. Andres, C. Gonzalez, M. Head-Gordon, E. S. Replogle, and J. A. Pople, Gaussian, Inc., Pittsburgh PA, 1998.

Table I Optimized geometries of the electronic states of M_4Na (M=Al, Ga, In) and their ions at the CASSCF level.

System	state		Geometry parameters						
	C_{2v}	C_{4v}	1-2	2-3	3-4	1-3	1-5	2-5	Figure
Al_4Na^-	$^1A_1$	$^1A_1$	2.619	2.619	2.619	3.703	3.342	3.342	(1a)
	$^1A_1$		2.643	2.546	2.585	3.573	3.000	3.000	(1d)
Al_4Na	$^2A_1$		2.584	2.584	2.584	3.027	3.283	3.555	(1c)
	$^2A_2$	$^2B_1$	2.612	2.612	2.612	3.694	3.401	3.401	(1a)
	$^4B_2$		2.711	2.711	2.711	2.643	3.242	3.715	(1c)
	$^2B_1$		2.662	2.608	2.645	3.720	3.086	3.086	(1d)
	$^2A_1$		2.569	2.600	2.546	3.647	3.067	3.067	(1d)
Al_4Na^+	$^1A_1$	$^1A_1$	2.645	2.645	2.645	3.741	3.641	3.641	(1a)
	$^1A_1$		2.617	2.617	2.617	2.760	3.441	3.974	(1c)
	$^3A_2$		2.616	2.616	2.616	2.854	3.456	3.884	(1c)
Ga_4Na^-	$^1A_1$	$^1A_1$	2.590	2.590	2.590	3.663	3.351	3.351	(1a)
	$^1A_1$		2.602	2.506	2.546	3.592	2.954	2.954	(1d)
Ga_4Na	$^2A_1$		2.603	2.603	2.603	3.681	3.463	3.463	(1a)
	$^2A_1$		2.543	2.644	2.543	3.669	3.445	3.445	(1b)
	$^2A_2$		2.600	2.600	2.600	3.677	3.438	3.438	(1a)
	$^4B_2$		2.711	2.711	2.711	2.678	3.229	3.738	(1c)
	$^2B_1$		2.623	2.575	2.627	3.677	3.043	3.043	(1d)
	$^2A_1$		2.529	2.567	2.522	3.601	3.018	3.018	(1d)
Ga_4Na^+	$^1A_1$	$^1A_1$	2.642	2.642	2.642	3.736	3.696	3.696	(1a)
	$^1A_1$		2.517	2.774	2.517	3.746	3.687	3.687	(1b)
	$^3A_2$		2.617	2.617	2.617	2.957	3.502	3.902	(1c)
In_4Na^-	$^1A_1$	$^1A_1$	2.937	2.937	2.937	4.154	3.571	3.571	(1a)
	$^1A_1$		2.942	2.840	2.897	4.073	3.137	3.137	(1d)
In_4Na	$^2A_1$		2.959	2.959	2.959	4.185	3.675	3.675	(1a)
	$^2A_2$		2.961	2.961	2.961	4.265	3.619	3.619	(1a)
	$^4B_2$		3.083	3.083	3.083	3.086	3.422	3.974	(1c)
	$^2B_1$		2.949	2.922	3.005	4.171	3.214	3.214	(1d)
	$^2A_1$		2.871	2.901	2.879	4.084	3.197	3.197	(1d)
In_4Na^+	$^1A_1$	$^1A_1$	3.007	3.007	3.007	4.253	3.851	3.851	(1a)
	$^1A_1$		2.876	3.132	2.876	4.252	3.852	3.852	(1b)
	$^3A_2$		2.986	2.986	2.986	3.398	3.674	4.067	(1c)

Table II Optimized geometries of the electronic states of M_4Na (M=Al, Ga, In) and their ions at the DFT level.

System		state	Geometry parameters						
	C_{2v}	C_{4v}	1-2	2-3	3-4	1-3	1-5	2-5	Figure
Al_4Na^-	$^1A_1$	$^1A_1$	2.616	2.616	2.616	3.700	3.180	3.180	(1a)
	$^1A_1$		2.664	2.525	2.585	3.642	2.973	2.973	(1d)
Al_4Na	$^2A_1$		2.608	2.608	2.608	3.256	3.201	3.374	(1c)
	$^2A_2$	$^2B_1$	2.624	2.624	2.624	3.710	3.272	3.272	(1a)
	$^4B_2$		2.707	2.707	2.707	2.682	3.159	3.490	(1c)
	$^2B_1$		2.714	2.582	2.647	3.722	3.047	3.047	(1d)
	$^2A_1$		2.608	2.593	2.608	3.654	3.013	3.013	(1d)
Al_4Na^+	$^1A_1$	$^1A_1$	2.679	2.679	2.679	3.789	3.499	3.499	(1a)
	$^1A_1$		2.633	2.633	2.633	2.940	3.351	3.696	(1c)
	$^3A_2$		2.637	2.637	2.637	2.999	3.355	3.650	(1c)
Ga_4Na^-	$^1A_1$	$^1A_1$	2.582	2.582	2.582	3.652	3.159	3.159	(1a)
	$^1A_1$		2.621	2.478	2.562	3.585	2.936	2.936	(1d)
Ga_4Na	$^2A_1$	$^2A_1$	2.599	2.599	2.599	3.676	3.268	3.268	(1a)
	$^2A_1$		2.575	2.624	2.575	3.676	3.269	3.269	(1b)
	$^2A_2$	$^2B_1$	2.601	2.601	2.601	3.679	3.262	3.262	(1a)
	$^4B_2$		2.716	2.716	2.716	2.740	3.125	3.547	(1c)
	$^2B_1$		2.666	2.546	2.666	3.676	3.008	3.008	(1d)
	$^2A_1$		2.561	2.555	2.561	3.602	2.969	2.969	(1d)
Ga_4Na^+	$^1A_1$	$^1A_1$	2.652	2.652	2.652	3.751	3.519	3.519	(1a)
	$^1A_1$		2.544	2.777	2.544	3.765	3.517	3.517	(1b)
	$^3A_2$		2.655	2.655	2.655	3.449	3.453	3.577	(1c)
In_4Na^-	$^1A_1$	$^1A_1$	2.926	2.926	2.926	4.138	3.354	3.354	(1a)
	$^1A_1$		3.004	2.878	2.993	4.156	3.176	3.176	(1d)
In_4Na	$^2A_1$	$^2A_1$	2.947	2.947	2.947	4.168	3.464	3.464	(1a)
	$^2A_2$	$^2B_1$	2.953	2.953	2.953	4.176	3.449	3.449	(1a)
	$^4B_2$		3.083	3.083	3.160	3.083	3.304	3.757	(1c)
	$^2B_1$		3.004	2.878	2.993	4.156	3.176	3.176	(1d)
	$^2A_1$		2.910	2.885	2.867	4.082	3.138	3.138	(1d)
In_4Na^+	$^1A_1$	$^1A_1$	3.011	3.011	3.011	4.258	3.673	3.673	(1a)
	$^1A_1$		2.923	3.104	2.923	4.263	3.672	3.672	(1b)
	$^3A_2$		3.022	3.022	3.022	4.274	3.666	3.666	(1c)

Table III Vibrational frequencies and IR intensities of the electronic states of M_4Na (M=Al, Ga, In) and their ions at the DFT level.

System	state		Vibrational frequencies (IR intensities)									Figure
	C_{2v}	C_{4v}										
Al_4Na^-	$^1A_1$	$^1A_1$	i195.7	27.2	84.8	105.8	128.9	156.1	249.2	277.1	291.1	(1a)
			(0.00)	(0.07)	(0.01)	(0.03)	(0.05)	(21.9)	(0.03)	(1.99)	(0.04)	
	$^1A_1$		28.5	69.0	104.2	145.4	172.6	258.9	302.0	323.5	352.5	(1d)
			(7.48)	(0.11)	(0.00)	(2.31)	(1.34)	(0.00)	(5.52)	(6.15)	(0.31)	
Al_4Na	$^2A_1$		60.3	89.0	115.1	134.4	171.5	214.2	254.5	287.9	292.7	(1c)
			(0.34)	(0.37)	(0.88)	(1.26)	(15.2)	(0.00)	(2.26)	(3.29)	(0.00)	
	$^2A_2$		85.4	85.7	98.3	134.9	161.0	236.2	236.3	281.7	449.0	(1a)
			(0.18)	(0.18)	(0.00)	(0.00)	(19.3)	(0.98)	(0.98)	(5.00)	(0.00)	
	$^4B_2$		59.9	64.4	91.7	143.8	169.2	222.4	249.4	268.1	285.6	(1c)
			(0.19)	(2.22)	(0.63)	(0.33)	(13.5)	(0.57)	(0.00)	(11.45)	(3.40)	
	$^2B_1$		24.1	61.9	72.9	148.8	163.1	238.9	282.6	294.3	335.5	(1d)
			(1.24)	(0.00)	(0.72)	(0.33)	(12.7)	(3.16)	(5.76)	(1.98)	(3.34)	
	$^2A_1$		i65.1	58.1	92.3	111.8	171.3	267.1	291.3	305.7	340.6	(1d)
			(1.10)	(102.6)	(0.00)	(0.84)	(18.4)	(0.11)	(0.09)	(6.90)	(3.01)	
Al_4Na^+	$^1A_1$	$^1A_1$	i78.3	i52.0	61.5	61.5	132.3	144.1	260.4	260.4	266.9	(1a)
			(0.00)	(0.00)	(0.01)	(0.01)	(14.4)	(0.00)	(0.04)	(0.04)	(0.27)	
	$^1A_1$		i195.5	27.4	84.9	105.9	128.9	156.2	249.1	276.9	290.9	(1c)
			(0.00)	(0.07)	(0.01)	(2.08)	(0.05)	(21.9)	(0.03)	(1.98)	(0.04)	
	$^3A_2$		50.7	79.4	94.8	144.4	154.7	188.6	252.9	270.8	295.3	(1c)
			(0.07)	(0.03)	(0.28)	(23.2)	(3.03)	(0.16)	(15.2)	(2.82)	(0.00)	
Ga_4Na^-	$^1A_1$	$^1A_1$	67.5	67.5	90.1	110.7	155.4	158.0	158.0	179.9	182.9	(1a)
			(0.17)	(0.17)	(0.00)	(0.00)	(4.38)	(0.00)	(0.00)	(3.19)	(0.00)	
	$^1A_1$		20.2	60.8	75.9	108.0	139.6	170.8	182.2	197.8	223.3	(1d)
			(4.31)	(0.06)	(0.00)	(0.61)	(0.27)	(0.01)	(3.89)	(0.72)	(0.05)	
Ga_4Na	$^2A_1$		i43.1	45.8	59.1	59.1	99.8	145.3	157.3	157.3	173.9	(1d)
			(0.00)	(0.00)	(0.86)	(0.86)	(0.00)	(11.5)	(0.02)	(0.02)	(0.28)	
	$^2A_1$		47.0	56.1	57.9	60.4	99.1	145.1	151.7	162.0	173.8	(1a)
			(0.00)	(0.81)	(0.23)	(0.90)	(0.00)	(11.6)	(0.13)	(0.00)	(0.31)	
	$^2A_2$		65.3	65.3	74.3	91.0	135.4	135.4	145.9	171.2	271.7	(1b)
			(0.48)	(0.48)	(0.00)	(0.00)	(2.47)	(2.47)	(16.9)	(0.50)	(0.00)	

	$^4B_2$		42.6	43.4	70.7	75.8	123.3	142.9	148.8	157.0	162.8	(1c)
			(0.45)	(0.32)	(1.05)	(0.20)	(10.5)	(0.00)	(12.2)	(10.5)	(0.36)	
	$^2B_1$		19.3	59.3	59.7	106.9	128.7	160.7	169.2	176.0	210.6	(1d)
			(0.47)	(0.00)	(1.23)	(0.33)	(0.29)	(9.03)	(2.84)	(0.01)	(6.35)	
	$^2A_1$		38.4	38.4	69.6	91.0	141.5	170.8	178.6	185.5	214.6	(1d)
			(1.10)	(48.9)	(0.00)	(1.23)	(3.37)	(3.09)	(0.52)	(6.23)	(9.04)	
Ga_4Na^+	$^1A_1$	$^1A_1$	i103.0	39.2	43.8	43.8	94.3	117.5	153.0	153.0	156.9	(1a)
			(0.00)	(0.00)	(0.99)	(0.99)	(0.00)	(18.2)	(0.56)	(0.56)	(0.01)	
	$^1A_1$		28.8	35.6	53.1	88.0	110.4	120.5	130.0	163.5	170.2	(1b)
			(0.00)	(0.63)	(1.08)	(0.00)	(8.85)	(10.7)	(1.97)	(0.00)	(1.05)	
	$^3A_2$		28.7	42.3	50.1	71.5	114.3	119.1	133.8	152.9	163.2	(1c)
			(0.05)	(0.45)	(0.88)	(0.02)	(1.54)	(23.4)	(6.40)	(0.11)	(0.00)	
In_4Na^-	$^1A_1$	$^1A_1$	56.5	62.9	62.9	71.8	105.2	105.2	115.8	122.5	140.7	(1a)
			(0.00)	(0.01)	(0.01)	(0.00)	(0.02)	(0.02)	(3.31)	(0.00)	(0.10)	
	$^1A_1$		15.0	41.8	48.1	86.0	99.1	121.4	130.3	133.3	169.4	(1d)
			(3.11)	(0.00)	(0.00)	(0.16)	(0.63)	(1.42)	(0.09)	(0.23)	(0.00)	
In_4Na	$^2A_1$		34.9	55.3	55.3	61.9	64.5	104.0	104.0	110.7	132.1	(1a)
			(0.00)	(0.33)	(0.33)	(0.00)	(0.00)	(0.10)	(0.10)	(2.90)	(3.85)	
	$^2A_2$		45.4	59.3	60.9	60.9	89.8	89.8	109.2	133.5	157.3	(1a)
			(0.00)	(0.00)	(0.08)	(0.08)	(1.82)	(1.82)	(5.34)	(5.80)	(0.00)	
	$^4B_2$		30.9	41.9	50.0	65.9	76.6	93.7	102.5	105.7	137.5	(1c)
			(0.14)	(0.00)	(0.05)	(0.65)	(0.07)	(0.00)	(2.33)	(6.81)	(4.68)	
	$^2B_1$		23.4	39.0	43.3	79.4	90.1	113.3	119.5	122.2	162.8	(1d)
			(2.38)	(0.00)	(0.43)	(0.29)	(0.30)	(1.71)	(0.05)	(1.30)	(10.8)	
	$^2A_1$		19.7	26.9	44.6	77.0	97.7	120.0	124.8	125.1	169.1	(1d)
			(13.4)	(0.47)	(0.00)	(0.69)	(0.11)	(0.53)	(0.68)	(1.74)	(14.7)	
In_4Na^+	$^1A_1$		i47.8	29.9	46.9	46.9	61.3	94.8	99.1	99.1	116.0	(1a)
			(0.00)	(0.00)	(0.47)	(0.47)	(0.00)	(3.46)	(0.69)	(0.69)	(9.70)	
	$^1A_1$		26.4	39.8	51.8	58.6	59.2	90.6	96.5	106.5	115.6	(1b)
			(0.00)	(0.28)	(0.57)	(0.76)	(0.00)	(1.27)	(3.61)	(0.83)	(9.73)	
	$^3A_2$		12.4	48.2	48.2	49.2	81.5	81.5	94.7	100.4	114.9	(1c)
			(0.00)	(0.14)	(0.14)	(0.00)	(2.66)	(2.66)	(5.51)	(0.00)	(11.2)	

Table IV Energy separations for the electronic states of M_4Na (M=Al, Ga, In) and their ions at the CASSCF, MRSDCI, MRSDCI+Q and DFT levels.

System	state		CASSCF	MRSDCI	MRSDCI+Q	DFT	
	C_{2v}	C_{4v}	E(eV)	E(eV)	E(eV)	E(eV)	Figure
Al_4Na^-	$^1A_1$	$^1A_1$	-0.810	-1.473	-1.441	-1.804	(1a)
	$^1A_1$		-0.610	-0.936	-1.176	-1.541	(1d)
Al_4Na	$^2A_1$		0.000	0.000	0.000	0.000	(1c)
	$^2A_2$	$^2B_1$	0.226	0.246	0.114	0.169	(1a)
	$^4B_2$		0.175	0.151	0.217	0.227	(1c)
	$^2B_1$		0.066	0.274	0.421	0.229	(1d)
	$^2A_1$		0.365	0.365	0.389	0.252	(1d)
Al_4Na^+	$^1A_1$	$^1A_1$	5.175	5.722	5.737	6.034	(1a)
	$^1A_1$		4.921	5.575	5.961	5.977	(1c)
	$^3A_2$		4.744	5.419	5.703	5.793	(1c)
Ga_4Na^-	$^1A_1$	$^1A_1$	-1.073	-1.604	-1.708	-1.747	(1a)
	$^1A_1$		-0.864	-1.089	-1.265	-1.489	(1d)
Ga_4Na	$^2A_1$	$^2A_1$	0.000	0.000	0.000	0.000	(1a)
	$^2A_1$		0.005	0.000	-0.081	0.000	(1b)
	$^2A_2$	$^2B_1$	0.016	0.084	0.242	0.140	(1a)
	$^4B_2$		0.004	0.234	0.277	0.373	(1c)
	$^2B_1$		-0.319	-0.062	0.097	0.202	(1d)
	$^2A_1$		0.013	0.250	0.327	0.240	(1d)
Ga_4Na^+	$^1A_1$	$^1A_1$	4.802	5.357	5.447	5.992	(1a)
	$^1A_1$		4.744	5.280	5.617	5.976	(1b)
	$^3A_2$		4.618	5.243	5.421	5.847	(1c)
In_4Na^-	$^1A_1$	$^1A_1$	-1.119	-1.685	-1.785	-1.754	(1a)
	$^1A_1$		-0.871	-1.080	-1.218	-1.454	(1d)
In_4Na	$^2A_1$	$^2A_1$	0.000	0.000	0.000	0.000	(1a)
	$^2A_2$	$^2B_1$	-0.055	0.079	0.103	0.149	(1a)
	$^4B_2$		-0.063	0.140	0.158	0.272	(1c)
	$^2B_1$		-0.275	-0.062	-0.145	0.190	(1d)
	$^2A_1$		0.100	0.278	0.282	0.289	(1d)
In_4Na^+	$^1A_1$	$^1A_1$	4.584	5.269	5.386	5.676	(1a)
	$^1A_1$		4.551	5.256	5.199	5.672	(1b)
	$^3A_2$		4.397	5.015	5.272	5.548	(1a)

Table V Computed energies for the various reaction pathways of M_4Na (M=Al, Ga, In) clusters and their ions at the MRSDCI and DFT levels

Dissociation paths	dissociation energies (eV)	
	MRSDCI	DFT
Al_4Na^- (C_{4v}, $^1A_1$) → Al_4^{2-} (D_{4h}, $^1A_{1g}$) + Na^+ (^1S)		8.504
Al_4Na^- (C_{4v}, $^1A_1$) → Al_4^- (D_{4h}, $^2A_{1g}$) + Na (^2S)	1.561	1.420
Al_4Na (C_{2v}, $^2A_1$) → Al_4 (C_{2v}, $^1A_1$) + Na (^2S)	1.799	1.984
Al_4Na^+ (C_{2v}, $^3A_2$) → Al_4 (C_{2v}, $^3A_1$) + Na^+ (^1S)	1.296	1.273
Ga_4Na^- (C_{4v}, $^1A_1$) → Ga_4^{2-} (D_{4h}, $^1A_{1g}$) + Na^+ (^1S)		8.591
Ga_4Na^- (C_{4v}, $^1A_1$) → Ga_4^- (D_{4h}, $^2A_{1g}$) + Na (^2S)	1.528	1.429
Ga_4Na (C_{4v}, $^2A_1$) → Ga_4 (D_{4h}, $^1A_{1g}$) + Na (^2S)	1.886	1.977
Ga_4Na^+ (C_{2v}, $^3A_2$) → Ga_4 (D_{4h}, $^3A_{1g}$) + Na^+ (^1S)	0.992	1.112
In_4Na^- (C_{4v}, $^1A_1$) → In_4^{2-} (D_{4h}, $^1A_{1g}$) + Na^+ (^1S)		8.307
In_4Na^- (C_{4v}, $^1A_1$) → In_4^- (D_{4h}, $^2A_{1g}$) + Na (^2S)	1.331	1.383
In_4Na (C_{4v}, $^2A_1$) → In_4 (D_{4h}, $^1A_{1g}$) + Na (^2S)	1.886	1.844
In_4Na^+ (C_{2v}, $^3A_2$) → In_4 (D_{4h}, $^3A_{1g}$) + Na^+ (^1S)	1.029	1.253
Al_4^- → Al_4^{2-}		1.667
Ga_4^- → Ga_4^{2-}		1.744
In_4^- → In_4^{2-}		1.506
IP_{Na}		5.417[a]

[a]Corresponding experimental value is 5.139 eV

Table VI Comparison of experimental, calculated vertical electron detachment energies (VDE) and vertical excitation energies in parentheses in eV at the DFT/B3LYP optimized geometries for Ga_4Na^- at the DFT/B3LYP, R(U)CCSD(T) and OVGF/6-311+G(2df)[a] levels

Expt	Symm	Calc VDE or vertical excitation energies		Expt	Excitation	Calc VDE
Features[a]	C_{4v}	DFT/R(U)B3LYP	R(U)CCSD (T)	VDE [a]	energies [a]	OVGF [a]
Ga_4Na^-	$^1A_1$	0.00 (-1.77)	0.00 (-1.87)	0.00	(-1.90)	0.00 (-1.84)
X	$^2A_1$	1.77 (0.00)	1.87 (0.00)	1.90	(0.00)	1.84 (0.00)
A	$^2B_1$	1.90 (0.13)	1.89 (0.02)	2.02	(0.12)	1.99 (0.15)
B	$^2A_1$	2.52 (0.75)	2.68 (0.81)	2.58	(0.68)	2.43 (0.59)
C	$^2B_2$	3.44 (1.68)	3.69 (1.82)	3.73	(1.83)	3.59 (1.75)

[a] From Ref. 15

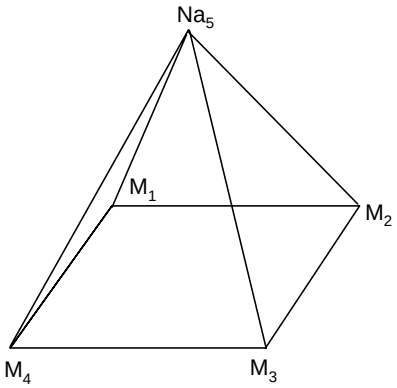

(a) and (b)

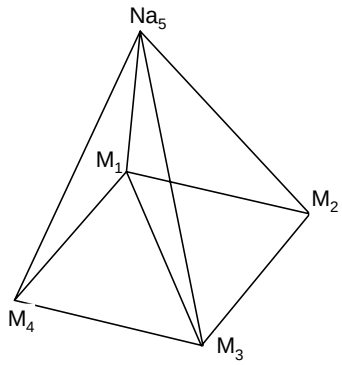

(c)

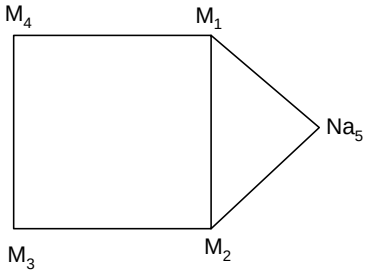

(d)

Figure Captions

Fig. 1 Possible geometries for the M_4Na (M=Al, Ga, In) clusters and their ions: (a) square pyramid (C_{4v}, bond distances M1-M2=M2-M3=M3-M4=M4-M1), (b) rectangular pyramid (C_{2v}, bond distances M1-M2=M3-M4≠M2-M3= M4-M1), and (c) rhomboidal pyramid (C_{2v}), and (d) Capped-square planar (C_{2v}).